Int. J. Heat Mass Transfer. Vol. 27, No. 5, pp. 647–655, 1984
Printed in Great Britain

0017-9310/84 \$3.00 + 0.00
Pergamon Press Ltd.

ANALYSIS OF SOLAR-DEHUMIDIFICATION DRYING†

B. PALÁNCZ‡

German Aerospace Research Establishment, Linder Höhe, D-5000 Köln 90, Federal Republic of Germany

(*Received* 2 *November* 1982 *and in revised form* 21 *March* 1983)

Abstract—A mathematical model for describing solar-dehumidification drying is presented. Lumped dynamical models have been applied to the moist material and to the solar collector. The other units of the drying system, drying chamber and dehumidifying heat-pump were considered to be in a quasi-steady state. The simulation of the weather conditions was carried out by a dynamical weather model. Drying operations under humidistat and temperature control with and without the solar collector were simulated. The analysis of the numerical study shows that although the drying time is not necessarily shorter in the case of solar-dehumidification drying than in that of simple dehumidification drying, the running time of the dehumidifier can be considerably reduced.

NOMENCLATURE

$\breve{a}, \breve{b}$	constants in equation (43), [dimensionless], [W m^{-2}], [(°C)^p], respectively
A	surface area [m^2]
$A_{1,2}, B_{1,2}, D_{1,2}$	constants in weather model, equations (62) and (63) [dimensionless]
c	specific heat [kcal kg^{-1} °C^{-1}]
c_L	constant in equation (64) [°C h^{-1}]
G	gas flow [kg h^{-1}]
h	enthalpy [kcal kg^{-1} (dry gas or dry solid)]
HR	solar radiation intensity [W m^{-2}]
$j_{1,2,3}$	control functions [dimensionless]
k	overall heat transfer coefficient [kcal m^{-2} h^{-1} °C^{-1}]
K	constant in equation (19) [dimensionless]
m	solid mass [kg (dry solid)]
(mc)	heat capacity [kcal °C^{-1}]
N	drying rate [kg (moisture) m^{-2} h^{-1}]
p	exponent in equation (43) [dimensionless]
p	partial pressure of moisture vapor in gas [mmHg]
q	heat flux [kcal m^{-2} h^{-1}]
Q_L	heat loss of drying chamber [kcal h^{-1}]
r_0	evaporation heat at 0°C [kcal kg^{-1}]
T	temperature [°C]
x	moisture content [kg (moisture) kg^{-1} (dry gas or dry solid)]
x_s^*	equilibrium humidity of gas contacting with solid surface [kg (moisture) kg^{-1} (dry gas)]
z	exponent for Lewis-factor [dimensionless].

Greek symbols

α	heat transfer coefficient [kcal m^{-2} h^{-1} °C^{-1}]
θ	time [h]
η	collector efficiency [dimensionless]
σ	evaporation coefficient [kg (dry gas) m^{-2} h^{-1}]
ϕ	relative humidity [dimensionless]
ψ	function representing sorptive property of moist solid [dimensionless]
ω	frequency factor [h^{-1}].

Indices

a	initial value
c	convective, critical, condenser, collector meaningfully
ch	collector heat exchanger
ci	collector inlet
co	collector outlet
cs	collector surface
E, E1, E2	evaporator, its cooling and dehumidifying section, respectively
i	inlet into drying chamber
o	outlet from drying chamber
p	leaving heat-pump or drying chamber
pwG	vapor at constant pressure
s	solid, surface, setpoint, meaningfully
w	moisture in liquid form
wG	humid gas
ws	moisture in vapor form
∞	ambient
$\tilde{()}$	space average
$\bar{()}$	time average.

Dimensionless factors

C	$2Gc_{wG}/k_{ch}A_{ch}$
Le	Lewis-factor, $\alpha_c/c_{wG}\sigma$
M	$2G/A_s\sigma$
P	$2Gc_{wG}/k_cA_c$.

† Dedicated to the 60th birthday of Prof. S. Szentgyörgyi.

‡ Present address: D-5000 Köln 51, Bonner Str. 401, Federal Republic of Germany.

1. INTRODUCTION

THE RECENT shortage in energy stimulated industrial and scientific research to find methods to cut energy consumption and to conserve energy as well as to explore new alternative energy sources.

Drying, as a thermal separation process, is an especially energy consuming process, because of the high evaporation heat of the moisture to be removed. To save the energy of the hot moist drying air, which is partly lost due to venting in the standard drying

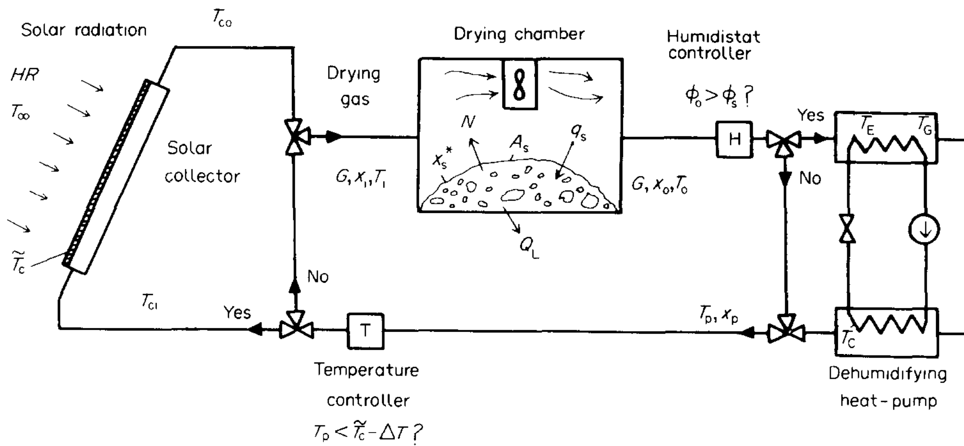

FIG. 1. Schematical diagram of a solar-dehumidifying dryer.

process, dehumidification drying was employed mainly in the wood-processing industry [1].

The alternative way, using other, possibly inexpensive and pollution-free energy sources for the drying process, was the application of solar dryers, where heat trapped by the external solar collector is supplied to the drying air circulating in the dryer [2].

To improve the efficiency both of dehumidification and solar drying, the two methods were combined [3]. The result of this marriage was a flexible, on weather conditions less dependent, economical drying process, namely solar-dehumidification drying. Figure 1 shows a schematical diagram of such a dryer. In the drying chamber the moisture content of the solid material is decreased through the convective drying process and the drying gas becomes moist. The relative humidity of the outlet air is measured. If it exceeds a preset value on the humidistat, the air is not returned directly but through the dehumidifier heat-pump. Here it is cooled down and the moisture removed by condensation. Then the cool, dry air is heated up in the condenser of the heat-pump. In the case where there is a low humidity content of the outlet air, the dehumidifier is bypassed. The air coming from the dehumidifier or directly from the drying chamber has two possible ways to return to the chamber-entrance. If its temperature is lower than that of the solar collector, it is blown through the collector and heated up. Otherwise the collector is bypassed.

The aim of this paper is to develop a simple mathematical model for the process, which can be employed for process simulation and in this way for analysing and designing solar-dehumidification drying processes as well as equipment.

2. MATHEMATICAL MODEL

A mathematical model of a solar-dehumidification dryer can be developed on the basis of the heat and mass balances applied to the different units of the system.

2.1. *Drying chamber*

If perfect mixing of the drying gas is supposed and neglecting its capacity terms in both of the balance equations, because they are usually small compared with that of the solid phase, the mass balance for the moisture content of the gas is

$$Gx_i + NA_s = Gx_o. \tag{1}$$

The moisture transport between the two phases, normally the evaporation or drying rate, may be expressed as

$$N = \sigma\left(x_s^* - \frac{x_i + x_o}{2}\right). \tag{2}$$

Combining equations (1) and (2) and arranging for x_o, one obtains

$$x_o = \frac{x_i(M-1) + 2x_s^*}{1+M}, \tag{3}$$

where

$$M = \frac{2G}{A_s\sigma}. \tag{4}$$

Similarly the quasi-steady state heat balance for the drying gas is

$$Gh_i + A_sNh_{ws} = Gh_o + A_sq_s + Q_L. \tag{5}$$

Considering that the enthalpy of the moist gas can be expressed as

$$h = c_{wG}T + r_0x, \tag{6}$$

and the moisture-enthalpy is

$$h_{ws} = r_0 + c_{pwG}T_s, \tag{7}$$

equation (5) can be written as

$$G(c_{wG}T_i + r_0x_i) + A_sN(r_0 + c_{pwG}T_s) = G(c_{wG}T_o + r_0x_o) + A_sq_s + Q_L. \tag{8}$$

Expressing the convective heat transfer between the solid and gas phase as

$$q_s = \alpha_c\left(\frac{T_i + T_o}{2} - T_s\right), \tag{9}$$

from equations (7) and (8) the temperature of the outlet gas is

$$T_o = \frac{M - Le^z}{M + Le^z} T_i + \frac{(r_0 + c_{pwG} T_s)(2x_s^* - x_i - x_o) + 2Le^z T_s c_{wG}}{c_{wG}(M + Le^z)} + \frac{M[r_0 G(x_i - x_o) - Q_L]}{Gc_{wG}(M + Le^z)}, \tag{10}$$

where

$$\frac{\alpha_c}{c_{wG}\sigma} = Le^z. \tag{11}$$

For the solid material to be dried a lumped model may be used. In this case the mass balance for its moisture content is

$$m_s \frac{dx_s}{d\theta} = -A_s N, \tag{12}$$

and the heat balance for the moist material can be written as

$$m_s \frac{dh_s}{d\theta} = A_s(q_s - N h_{ws}). \tag{13}$$

Considering that the enthalpy of the moist solid can be expressed as

$$h_s = (c_s + c_w x_s) T_s, \tag{14}$$

and employing equation (7), one may obtain

$$\frac{m_s}{A_s}(c_s + c_w x_s)\frac{dT_s}{d\theta} = q_s - N[r_0 + (c_{pwG} - c_w)T_s]. \tag{15}$$

The equilibrium moisture concentration in the drying gas having direct contact with the surface of the solid phase x_s^*, can be expressed as a function of the temperature and moisture content of the solid material. In general

$$x_s^* = x_s^*(T_s, x_s). \tag{16}$$

A usual form of equation (16) can be given for the air–water system as

$$\log p_{ws}^* = 0.622 + \frac{7.5T_s}{238 + T_s}, \tag{17}$$

and

$$x_s^* = 0.622 \frac{p_{ws}^*}{760 - p_{ws}^*} \psi(x_s). \tag{18}$$

Here $\psi(x_s)$ represents the sorptive property of the moist solid. In case the moisture content is under the critical value, x_{sc}

$$\psi(x_s) = \frac{x_s^n}{K + x_s^n} \quad \text{for} \quad x_s < x_{sc}, \tag{19}$$

otherwise $\psi = 1$.

Then equations (2), (3), (9), (10), (12), (15) and (17)–(19) under the initial conditions at $\theta = \theta_a$

$$x_s(\theta_a) = x_{sa}, \tag{20}$$

$$T_s(\theta_a) = T_{sa}, \tag{21}$$

and

$$x_o(\theta_a) = x_{oa}, \tag{22}$$

$$T_o(\theta_a) = T_{oa}, \tag{23}$$

describe the drying process in the drying chamber.

2.2. *Dehumidifier*

The next unit of the system is the dehumidifier. For the evaporator of the dehumidifying heat-pump, a quasi-steady distributed parameter model can be employed. In the first section of the evaporator, the moist gas will be cooled down to its dew-point. It means that in this section the moisture content of the gas remains constant and a simple gas-cooling process occurs. The mass balance for moisture in this section is

$$\frac{dx_G}{d\eta} = 0 \quad \text{if} \quad x_G < x_G^*(T_G), \tag{24}$$

where

$$\eta = \frac{A}{A_E} \quad \text{and} \quad 0 \leqslant \eta \leqslant 1. \tag{25}$$

The heat balance is

$$Gc_{wG}\frac{dT_G}{d\eta} = k_{E1}(T_E - T_G)A_E, \tag{26}$$

and the saturated moisture concentration can be computed from

$$x_G^* = 0.622\frac{p_G^*}{760 - p_G^*}, \tag{27}$$

where

$$\log p_G^* = 0.622 + \frac{7.5T_G}{238 + T_G}. \tag{28}$$

The second section starts where at the first time $x_G = x_G^*$. In this section the moist gas is supposed to be cooled down along the saturation-curve of the air–water system and a part of its moisture content condenses, so the gas is dehumidified.

The mass balance for this section is

$$x_G \equiv x_G^*(T_G), \tag{29}$$

and the heat balance can be written as

$$G\frac{dh_G}{d\eta} = k_{E2}(T_E - T_G)A_E, \tag{30}$$

or

$$c_{wG}\frac{dT_G}{d\eta}+r_0\frac{dx_G}{d\eta}=\frac{k_{E2}A_E}{G}(T_E-T_G). \quad (31)$$

Differentiating equation (29) and using equations (27) and (28) one obtains

$$\frac{dx_G}{d\eta}=f^*(T_G)\frac{dT_G}{d\eta}, \quad (32)$$

where

$$f^*(T_G)=\frac{0.622\times 238\times 760\times \ln 10\times 7.5}{[(760-p_G^*)(238+T_G)]^2}p_G^*, \quad (33)$$

and p_G^* can be computed from equation (28).

Then the heat balance equation has the following form

$$(c_{wG}+r_0f^*(T_G))\frac{dT_G}{d\eta}=\frac{k_{E2}A_E}{G}(T_E-T_G). \quad (34)$$

The boundary conditions are

$$T_G(\eta)_{\eta=0}=T_o(\theta), \quad (35)$$

$$x_G(\eta)_{\eta=0}=x_o(\theta). \quad (36)$$

In the condenser the gas is warmed-up, that is why its humidity remains constant. Then a simple heat balance may be written for the humid gas as

$$Gc_{wG}(T_p-T_{G1})=k_cA_c\left(T_c-\frac{T_p+T_{G1}}{2}\right), \quad (37)$$

where

$$T_{G1}=T_G(\eta)_{\eta=1}. \quad (38)$$

From equation (37) the temperature of the drying gas leaving the dehumidifier can be expressed as

$$T_p=\frac{2T_c+(P-1)T_{G1}}{1+P}, \quad (39)$$

where

$$P=\frac{2Gc_{wG}}{k_cA_c}, \quad (40)$$

and its moisture content is

$$x_p=x_G(\eta)_{\eta=1}. \quad (41)$$

2.3. *Solar collector*

Last but not least, the solar collector unit is considered. The heat balance for the collector may be written as

$$Gc_{wG}(T_{co}-T_{ci})+(mc)_c\frac{d\tilde{T}_c}{d\theta}=\eta_c(HR)A_c, \quad (42)$$

where the collector efficiency, η_c, can be approximated as [4]

$$\eta_c=\breve{a}-\breve{b}(\Delta\tilde{T})^p/HR, \quad (43)$$

and

$$\Delta\tilde{T}=\tilde{T}_c-T_\infty. \quad (44)$$

In case the collector is bypassed but the solar radiation is not zero, one obtains

$$(mc)_c\frac{d\tilde{T}_c}{d\theta}=HR\left(\breve{a}-\breve{b}\frac{\Delta\tilde{T}^p}{HR}\right)A_c. \quad (45)$$

When the intensity of the solar radiation is zero, the heat balance is

$$(mc)_c\frac{d\tilde{T}_c}{d\theta}=k_{cs}(T_\infty-\tilde{T}_c)A_c. \quad (46)$$

The outlet temperature of the drying gas T_{co} can be determinated in the following way

$$Gc_{wG}(T_{co}-T_{ci})=k_{ch}A_{ch}\left(\tilde{T}_c-\frac{T_{co}+T_{ci}}{2}\right), \quad (47)$$

and therefore

$$T_{co}=\frac{(C-1)T_{ci}+2\tilde{T}_c}{C+1}, \quad (48)$$

where

$$C=\frac{2Gc_{wG}}{k_{ch}A_{ch}}. \quad (49)$$

In case the collector is bypassed, the drying gas temperature does not change

$$T_i=T_{ci}. \quad (50)$$

Because the moisture content of the drying gas is independent from the fact, whether the gas stream flows through the collector or is bypassed, it can be written that

$$x_i=x_p. \quad (51)$$

3. CONTROL ACTIONS

The control actions among these three units have now to be defined. The dehumidifier is activated whenever the relative humidity of the gas leaving the dryer exceeds the preset value on the humidistat. This means that T_p and x_p are computed on the basis of the dehumidifying heat-pump model if $\phi_o \geq \phi_s$, but otherwise

$$T_p=T_o, \quad (52)$$

$$x_p=x_o. \quad (53)$$

That is why the humidistat control action is

$$j_1(\theta)=\begin{cases}1 & \text{if} \quad \phi_o\geq\phi_s,\\ 0 & \text{if} \quad \phi_o<\phi_s,\end{cases} \quad (54)$$

where $j_1=1$, the dehumidifier is activated and where $j_1=0$, the dehumidifier is bypassed.

The relative humidity of the drying gas can be calculated as

$$\phi_o=\frac{p_o}{p_o^*}, \quad (55)$$

where

$$p_o = 760\frac{x_o}{0.622+x_o}, \quad (56)$$

and

$$\log p_o^* = 0.622+\frac{7.5T_o}{238+T_o}. \quad (57)$$

In case the collector temperature $\tilde{T}_c$ exceeds T_p plus a prespecified ΔT value, then the collector circuit is activated and T_{co} calculated from the collector model. Therefore

$$T_i = T_{co}, \quad (58)$$

otherwise

$$T_i = T_p. \quad (59)$$

Then the control action of the temperature controller is

$$j_2(\theta) = \begin{cases} 1 & \text{if} \quad \tilde{T}_c > T_p+\Delta T, \\ 0 & \text{otherwise,} \end{cases} \quad (60)$$

where $j_2 = 1$, the collector circuit is activated and where $j_2 = 0$, the collector is bypassed.

The radiation controller is not a physical unit, it is a part of the simulation model. Its action is as follows

$$j_3(\theta) = \begin{cases} 1 & \text{if} \quad HR(\theta) > 0, \\ 0 & \text{if} \quad HR(\theta) = 0, \end{cases} \quad (61)$$

where

$$j_3 = 0,$$

collector heat balance is represented by equation (46), where

$$j_3 = 1 \quad \text{and} \quad j_2 = 0,$$

collector heat balance is represented by equation (45), and where

$$j_3 = 1 \quad \text{and} \quad j_2 = 1,$$

collector heat balance is represented by equation (42).

4. WEATHER MODEL

To simulate the weather conditions, the following formulae are employed for approximating the ambient temperature $T_\infty(\theta)$ and radiation intensity $HR(\theta)$

$$T_\infty(\theta) = \bar{T}_\infty[A_1\cos(\omega\theta)+B_1\sin(\omega\theta)+D_1], \quad (62)$$

and

$$HR(\theta) = \overline{HR}[A_2\cos(\omega\theta)+B_2\sin(\omega\theta)+D_2]. \quad (63)$$

When more than one day is simulated, the constants, A_i, B_i and D_i may change day to day.

The decrease of the ambient temperature after sunset may be taken into consideration as

$$\frac{dT_\infty}{d\theta} = -c_L \quad \text{if} \quad \theta_{set} \leqslant \theta \leqslant \theta_{rise}, \quad (64)$$

and

$$HR(\theta) = 0. \quad (65)$$

5. SIMULATION OF THE PROCESS

The mathematical model described above was transformed into a computer code and a digital simulation of the process was carried out according to Fig. 2 using the data set presented in Table 1.

The results of the simulation are shown on Figs. 3–17.

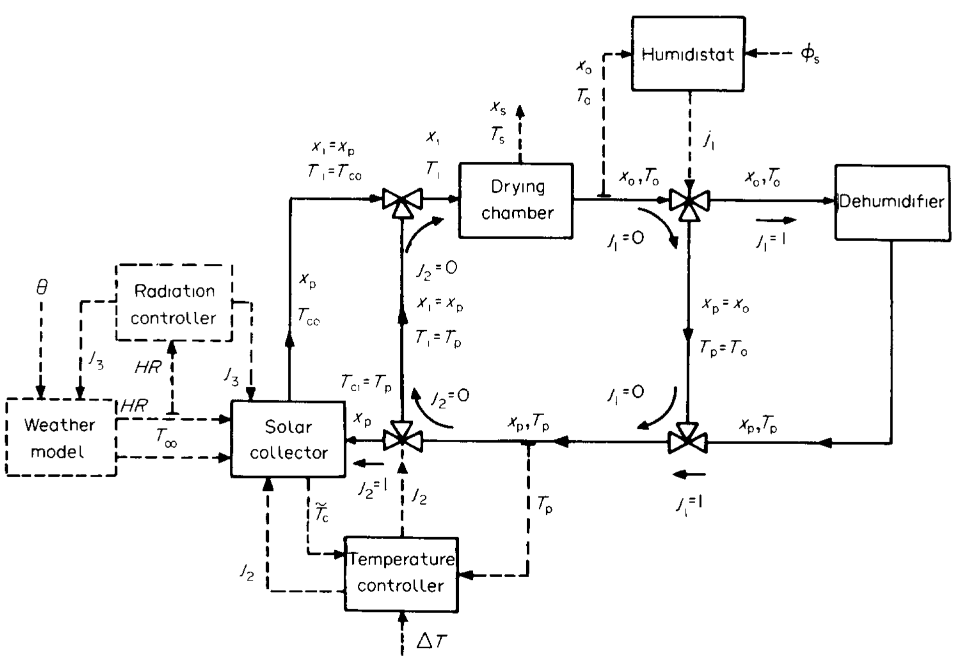

FIG. 2. Simulation model.

Table 1. Data for process simulation

$\theta_a = 8.5$ h	$c_{pwG} = 0.46$ kcal kg^{-1} °C^{-1}	$k_{E2} = 15$ kcal m^{-2} h^{-1} °C^{-1}	$k_{cs} = 5$ kcal m^{-2} h^{-1} °C^{-1}
$x_i(\theta_a) = 0.0134$	$r_0 = 597$ kcal kg^{-1}	$T_c = 55$°C	$C = 3.2$
$T_i(\theta_a) = 20$°C	$z = 1$	$P = 1.6$	$\bar{T}_\infty = 10$°C
$G = 1000$ kg h^{-1}	$Le = 1$	$\phi_s = 0.8$–0.2	$A_1 = -2.3654$
$x_{oa} = 0.0134$	$\alpha_c = 10$ kcal m^{-2} h^{-1} °C^{-1}	$\Delta T = 15$°C	$B_1 = -0.24$
$T_{oa} = 20$°C	$\sigma = 40$ kg m^{-2} h^{-1}	$\tilde{T}_{ca} = 20$°C	$D_1 = -0.7504$
$x_{sa} = 0.6$	$x_{sc} = 0.2$	$T_{\infty a} = 5$°C	$\overline{HR} = 200$ W m^{-2}
$T_{sa} = 20$°C	$c_{wG} = 0.26$ kcal kg^{-1} °C^{-1}	$(HR)_a = 190.3$ W m^{-2}	$A_2 = -2.765$
$m_s = 200$ kg	$n = 3$	$(mc)_c = 80$ kcal °C^{-1}	$B_2 = 0$
$A_s = 20$ m^2	$K = 0.001$	$\breve{a} = 0.783$	$D_2 = -1.0465$
$Q_L = 0$ kcal h^{-1}	$A_E = 10$ m^2	$\breve{b} = 0.028$ W (°C)$^{-p}$ m^{-2}	$\omega = 0.2618$ h^{-1}
$c_s = 0.5$ kcal kg^{-1} °C^{-1}	$T_E = 15$°C	$p = 1.15$	$c_L = 0.05$°C h^{-1}
$c_w = 1$ kcal kg^{-1} °C^{-1}	$k_{E1} = 15$ kcal m^{-2} h^{-1} °C^{-1}	$A_c = 10$ m^2	

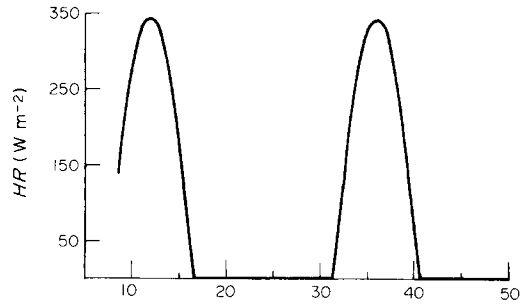

FIG. 3. Solar radiation intensity vs time, simulated by the weather model.

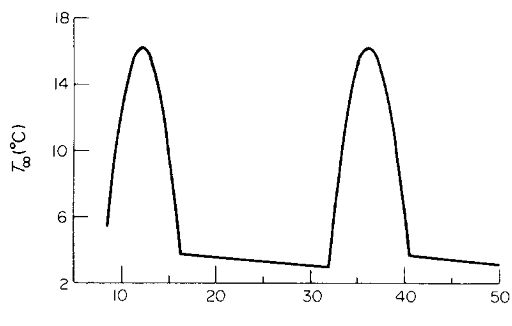

FIG. 4. Ambient temperature history.

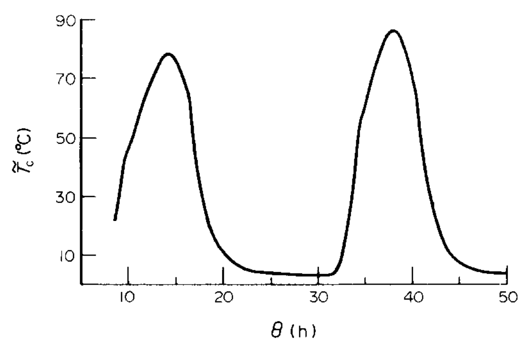

FIG. 5. Collector average temperature vs time.

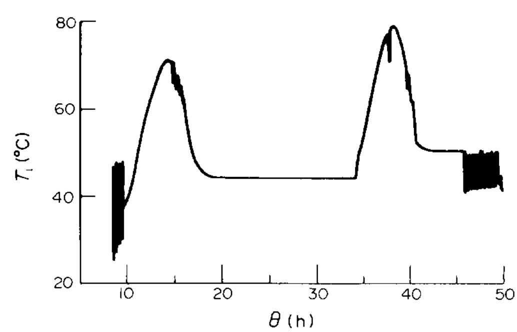

FIG. 6. Temperature of drying gas entering the dryer as a function of time in the case $\phi_s = 0.8$ and $A_c = 10$ m^2.

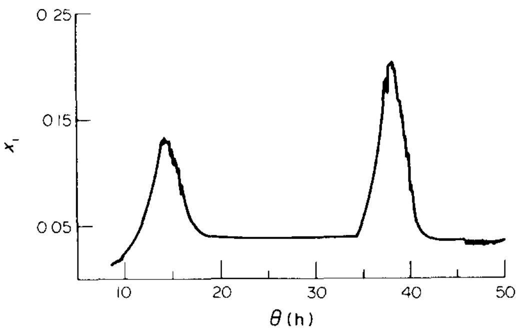

FIG. 7. Humidity content of drying gas entering the dryer as a function of time in the case $\phi_s = 0.8$ and $A_c = 10\ m^2$.

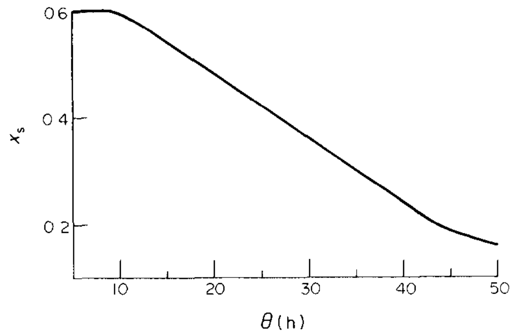

FIG. 11. Moisture content of solid material as a function of time in the case of $\phi_s = 0.8$ and $A_c = 0\ m^2$.

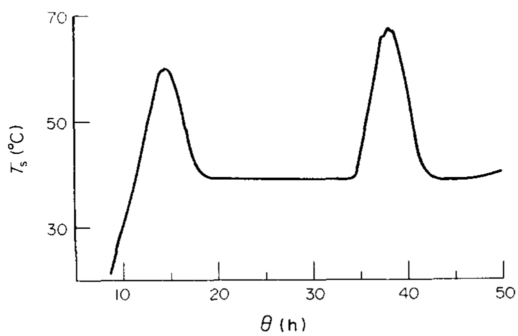

FIG 8. Temperature of solid material as a function of time in the case of $\phi_s = 0.8$ and $A_c = 10\ m^2$.

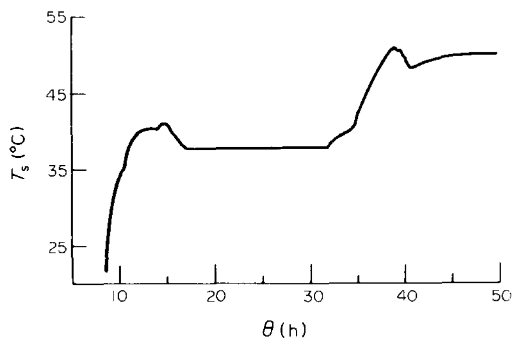

FIG. 12. Temperature of solid material as a function of time in the case of $\phi_s = 0.2$ and $A_c = 10\ m^2$.

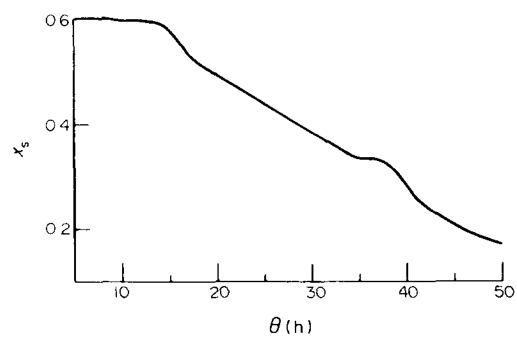

FIG. 9. Moisture content of solid material as a function of time, in the case of $\phi_s = 0.8$ and $A_c = 10\ m^2$.

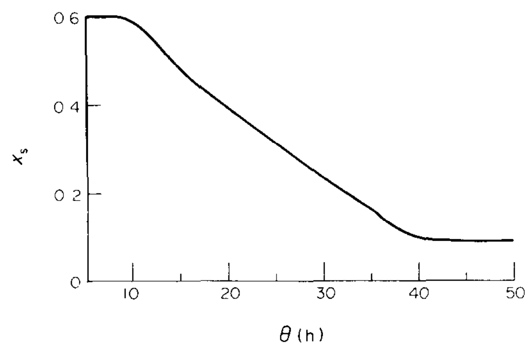

FIG. 13. Moisture content of solid material as a function of time in the case of $\phi_s = 0.2$ and $A_c = 10\ m^2$.

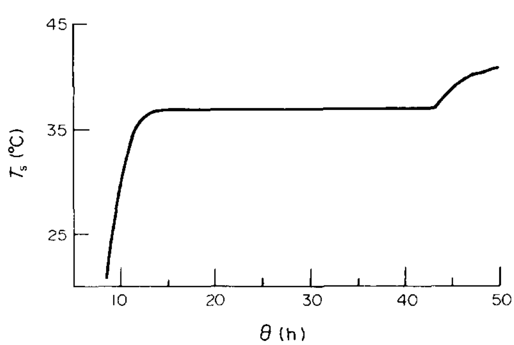

FIG. 10. Temperature of solid material as a function of time in the case of $\phi_s = 0.8$ and $A_c = 0\ m^2$.

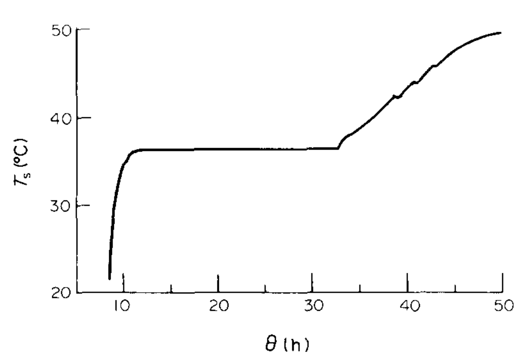

FIG. 14. Temperature of solid material as a function of time in the case of $\phi_s = 0.2$ and $A_c = 0\ m^2$.

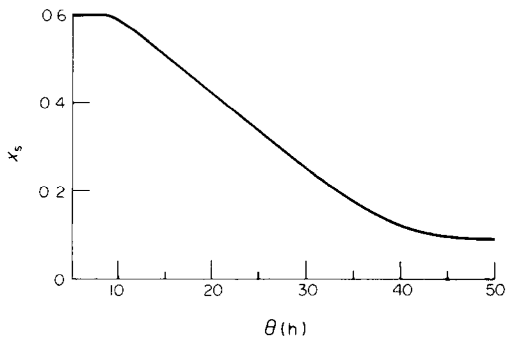

FIG. 15. Moisture content of solid material as a function of time in the case of $\phi_s = 0.2$ and $A_c = 0$.

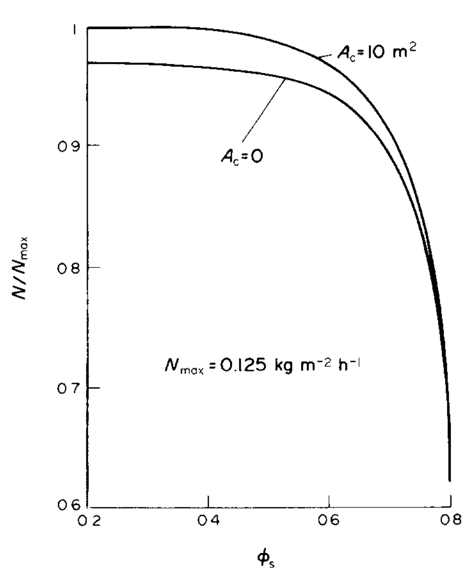

FIG. 16. The relative average drying rate as a function of the humidistat set-point with and without the solar collector.

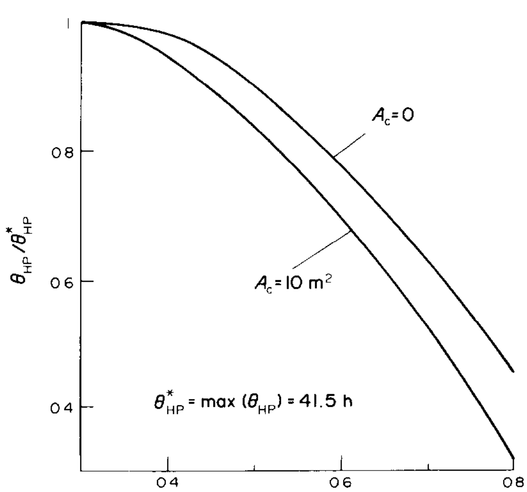

FIG. 17. The relative total working time of the dehumidifier as a function of the humidistat set-point, with and without the solar collector.

Figures 3 and 4 show the solar radiation and ambient temperature history.

At the beginning of the process the collector is not activated and its temperature increases rapidly (Fig. 5). Because of the high set-point value of the humidistat, $\phi_s = 0.8$, the dehumidifier operates bang-bang way.

In this warm-up period the condenser temperature is considerably higher than that of the moist solid material. That is why, this bang-bang operation mode causes a strong oscillation in the temperature of the gas entering the drying chamber (Fig. 6). On the other hand, the evaporator temperature is not low enough to dehumidify effectively the drying gas leaving the chamber. Therefore, the drying rate is practically zero (Fig. 9) and only a very small oscillation appears in the entering gas humidity (Fig. 7).

When the collector has reached a temperature, high enough to be activated, the gas in it will be heated up further and the heat-pump is less frequently on.

Consequently the collector temperature is elevated slower, the temperature oscillation ceases and the absolute inlet gas humidity increases. The temperature of the solid material also increases (Fig. 8), but remains behind the steady-state equilibrium temperature belonging to the actual inlet gas state. This fact combined with the high humidistat set-point, results in a very low drying rate (Fig. 9).

When the collector temperature decreases, the dehumidifier will be more frequently in operation. Now oscillation appears again in both state variables of the inlet drying gas (Figs. 6 and 7).

Further on the collector will be bypassed and the system reaches a steady-state with a higher drying rate (Figs. 6–9).

In the next time period, the situation is similar except the higher maximum temperature of the collector. It is because now the solid and gas temperature are higher than they were at the beginning of the process. When the moisture content of the solid material is below the critical value, oscillation in the temperature and humidity content of the inlet gas occurs again.

After that, the fact demonstrated by Figs. 10 and 11 is not very surprising. Namely, without the collector the drying process is much more 'smooth' and may be a little bit more efficient, too. However, reducing the set-point of the humidistat to $\phi_s = 0.2$ leads to a considerable change in the process variables (Figs. 12 and 13).

Now the temperature and moisture content history of the solid are much more similar to that of a normal batch drying process carried out with constant inlet gas temperature and humidity.

One can also see that using the solar collector, the intensity of the drying process may be improved (Figs. 12–15).

Figure 16 shows how the average drying rate changes as a function of ϕ_s with and without the collector. According to Fig. 16 the collector does not improve the dryer performance at high humidistat set-point values.

However, the use of the solar collector can result in an efficient reduction in the total working time of the dehumidifyer heat-pump at higher ϕ_s values (Fig. 17).

6. CONCLUSION

A mathematical model for analysing a solar batch dehumidifying drying process has been developed and was studied by computer simulation. The numerical results show that although the drying time cannot be reduced considerably, the total heat-pump working time is lower than with simple dehumidifying driers. The computations also indicate that the humidistat set-point has a very significant effect on the drying process.

These conclusions are in good agreement with the experimental findings [3].

However, to make the model more sophisticated and to analyse other control techniques than the bang-bang one, it would be recommended to improve the drying model applied to the moist solid as well as to take into consideration the time delay caused by the pipe system connecting the units.

REFERENCES

1. M. Y. Cech and F. Pfaff, Dehumidification drying of spruce studs, *Forest Prod. J.* **28**, 22–26 (1978).
2. H. N. Rosen and P. Y. S. Chen, Drying lumber in a kiln with external solar collectors, *New process alternatives in the forest products industries, A.I.Ch.E. Symp. Ser.* **76**, 82–89 (1980).
3. P. Y. S. Chen, W. A. Helmer and H. N. Rosen, Experimental studies of solar and solar-dehumidification lumber drying, *J. Energy* **5**, 130–131 (1981).
4. H. Tabor, Testing of solar collectors, *Solar Energy* **20**, 293–303 (1978).

ANALYSE DU SECHAGE SOLAIRE

Résumé—On présente un modèle pour décrire le séchage solaire. Des modèles dynamiques modulaires sont appliqués au matériau humide et au collecteur solaire. Les autres parties du système, chambre de séchage et pompe à chaleur de déshumidification sont considérées en état quasi stationnaire. La simulation des conditions climatiques est réalisée par un modèle dynamique. Des opérations de séchage sous contrôle d'humidité et de température avec ou sans le collecteur solaire sont simulées. L'analyse de l'étude numérique montre que bien que la durée du séchage ne soit pas nécessairement plus courte dans le cas du séchage solaire que dans celui d'un simple séchage, le temps de fonctionnement du déshumidificateur peut être considérablement réduit.

UNTERSUCHUNG DER SOLAREN ENTFEUCHTUNGSTROCKNUNG

Zusammenfassung—Ein mathematisches Modell, das die solare Entfeuchtungstrocknung beschreibt, wird vorgelegt. Für das feuchte Gut und den Sonnenkollektor wurden kombinierte dynamische Modelle angewandt. Die übrigen Komponenten des Trocknungssystems, die Trocknungskammer und die Entfeuchtungswärmepumpe wurden als quasistationär betrachtet. Die Simulation der Wetterbedingungen wurde mit einem dynamischen Wettermodell durchgeführt. Es wurden Trocknungsvorgänge mit Feuchtigkeits- und Temperaturüberwachung mit und ohne Sonnenkollektor simuliert. Die Analyse der numerischen Berechnung zeigt, daß—obwohl die Trocknungszeit im Fall der solaren Entfeuchtungstrocknung nicht unbedingt kürzer sein muß als bei einfacher Entfeuchtungstrocknung—die Betriebszeit des Entfeuchters beträchtlich reduziert werden kann.

АНАЛИЗ ПРОЦЕССА СУШКИ С ИСПОЛЬЗОВАНИЕМ СОЛНЕЧНОЙ ЭНЕРГИИ

Аннотация—Представлена математическая модель процесса сушки с использованием солнечной энергии. Для описания влажного материала и солнечного коллектора используются эквивалентные динамические модели. Предполагается, что остальные части системы, а именно сушильная камера и осушающий тепловой насос, работают в квазистационарном режиме. Погодные условия описываются с помощью динамической модели погоды. Проводится моделирование процессов сушки при регулировании влажности и температуры в системах с солнечным коллектором и без него. Анализ результатов численного исследования показывает, что хотя солнечная энергия и не обязательно ускоряет процесс сушки по сравнению с обычным обезвоживанием, тем не менее время работы осушителя может быть значительно сокращено.